

Equilibrium and Kinetics of Adsorption of Methylene Blue on Ti-Modified Volcanic Ashes

P. Esparza

Inorganic Chemistry Dept., University of La Laguna, Avda. Astrofísico Fco. Sánchez s/n, La Laguna, Tenerife, Canary Island 38200, Spain

M. E. Borges and L. Díaz

Chemical Engineering Dept., University of La Laguna, Avda. Astrofísico Fco. Sánchez s/n, La Laguna, Tenerife, Canary Island 38200, Spain

M. C. Alvarez-Galván and J. L. G. Fierro

Institute of Catalysis and Petroleum Chemistry, CSIC, C/ Marie Curie 2, Cantoblanco, 28049 Madrid, Spain

DOI 10.1002/aic.12285

Published online May 27, 2010 in Wiley Online Library (wileyonlinelibrary.com).

Volcanic ashes (VAs) and Ti-modified volcanic ashes (TVA) were investigated as inexpensive adsorbents to remove methylene blue (MB) from aqueous solutions. TVA displayed higher and faster MB adsorption than VA. Adsorption studies were carried out in a batch system at room temperature. In this work, several variables were studied: contact time, pH, initial MB concentration, and adsorbent dosage. The equilibrium data of MB adsorption were analyzed according to the Langmuir and Freundlich adsorption isotherm models. Optimum adsorption performance for TVAs particles, prepared using a hydrothermal method, was obtained at pH = 10 and 3 g/l adsorbent dose. MB adsorption isotherm data can be described satisfactorily by the Langmuir equation, whereas adsorption kinetic data fit a pseudo second-order kinetics model. © 2010 American Institute of Chemical Engineers AIChE J, 57: 819–825, 2011

Keywords: dyes, methylene blue, adsorption isotherm, kinetic model, volcanic ashes, nanomaterials

Introduction

The removal of organic dyes in waste effluents is of great environmental importance because they are widely used in industries such as textiles, paper, rubber, plastics, and cosmetics.^{1–3} In these industries, the color produced by organic dyes in water is esthetically unpleasant, it can affect plant life, and ecosystems become slowly destroyed. All these effects dictate the necessity of dye-containing water to undergo some treatment before its disposal to the environment. Many conventional treatment technologies for dye re-

moval have been investigated extensively such as chemical coagulation or flocculation combined with flotation and filtration, membrane filtration, oxidation, and photodegradation processes^{4,5}; however, these processes are not always effective and economics when dye concentrations are very low. Besides, most of the synthetic organic dyes undergo very slow biodegradation. Dye adsorption process provides an attractive method for the treatment of industrial effluents especially if the adsorbent is inexpensive, readily available,⁶ and does not require any expensive additional pretreatment step. Adsorption onto activated carbon is one of the most effective and reliable physicochemical processes for dyes-contaminated waste water treatment.^{7–9} Activated carbon has very high surface area, high adsorption capacity, and high degree of surface reactivity.¹⁰ However, activated carbon is

Correspondence concerning this article should be addressed to P. Esparza at pesparza@ull.es.

considered an expensive material, which limits its usage. This has led to a search for cheap and effective substitutes.¹¹ A number of low-cost adsorbents are reported in the literature. These include coal, fly ash, clay materials, zeolites, siliceous materials, agricultural wastes, and industrial waste products.^{12–19}

In this study, natural volcanic ashes (VAs) particles from volcanic lava soil occurring in the Canary Islands were used as adsorbent for the removal of methylene blue (MB) from an aqueous solution. This natural and very cheap material appears to be a promising adsorbent candidate for the removal of organic dyes.

MB was selected as a model compound to evaluate the capacity of VAs material as adsorbent for the removal of dyes from aqueous solutions. MB is a cationic dye whose molecular formula is $C_{16}H_{18}N_3SCl$. Although this molecule is not strongly hazardous, it can cause some harmful effects.²⁰

MB is widely used in coloring paper, dyeing cottons, wools, coating for paper stocks, etc. Its adsorption characteristics on various adsorbents have been extensively investigated for many purification and separation purposes. However, most of the previous works were focused in the use of activated carbons as adsorbent material for MB removal from waste waters.^{21–26} Some other studies were conducted by using natural zeolites,²⁷ fly ash,^{12,28} and agricultural wastes.^{16,20,29,30} Cost effectiveness, availability, and adsorptive properties are the main criteria taken into consideration for choosing an adsorbent that could be effective for the removal of organic compounds.

This work was undertaken with the aim to investigate the adsorption of MB onto Ti-containing VA, which is a low-cost adsorbent and it could be effective for dyes removal from waste water. Natural VAs particles were modified by TiO_2 impregnation to enhance their adsorption capacity by developing new micro- and nanostructures with subsequent increase in the surface area. Effects of contact time, adsorbent dose, initial dye concentration, and pH were evaluated. Adsorption isotherms, kinetics, and factors controlling the adsorption process were also evaluated and discussed.

Experimental

Natural VAs, from volcanic zone soil in Tenerife (Canary Islands), were ground and sieved (200–400 μm).³¹ The impregnation of these particles with TiO_2 was carried out using a hydrothermal method.^{32,33} Five grams of TiO_2 Merck and 25 g of natural VAs were added to a 50 ml of 1.0 M NaOH aqueous solution. The resulting suspension was heated at 140°C for 22 h in a teflon container, which was backed up by a stainless steel pressurized vessel. After hydrothermal treatment, the impregnated VA particles were washed with 0.1 M HCl solution and distilled water until pH 7 was reached. The impregnated material was then dried in air at 100°C for 15 min and heated at 140°C for 22 h in an oven.

The morphology of impregnation VAs was revealed by scanning electron microscopy (SEM, JEOL Model JSM-6300). The specific surface area and pore structure of samples were evaluated from nitrogen adsorption–desorption isotherms recorded at $-196^\circ C$ on a surface pore size analyzer (Gemini V, Micromeritics).

In equilibrium adsorption experiments, the effects of solution pH, adsorbent dose, and initial MB concentration were investigated. For each experiment, an amount of adsorbent and 800 ml of MB solution at a certain initial concentration and pH were introduced in a cylindrical flask. The mixture inside the flask was maintained in suspension by magnetic stirring at 1000 rpm. Once adsorption equilibrium was reached, the solid particles were removed by centrifugation. The concentration of the supernatant MB solution was determined using a UV/visible spectrophotometer (Varian Model Cary 50) at the MB maximum wavelength ($\lambda = 664$ nm). Subsequently, the concentration of dye was calculated from a calibration curve.

All the experiments were performed using a 20 mg/l initial dye concentration and 20°C. The initial pH of the solution was adjusted with HCl or NaOH. The effect of adsorbent dosage on the amount of MB adsorbed was studied by varying the Ti-loaded volcanic ashes (TVAs) particles dose between 0.5 and 20 g/l in the test solution. The pH of the dye solution plays an important role in the whole adsorption process, particularly on adsorption capacity.¹² To study the effect of pH on MB adsorption, experiments at three different pH values (3, 7, and 10) were carried out. The effect of MB initial solution concentration was studied within the concentration range 5–40 mg/l.

During adsorption studies, residual MB concentration was spectrophotometrically monitored, and the amount of MB adsorbed on the TVAs can be calculated as follows:

$$q_t = \frac{V(C_0 - C_t)}{m}, \quad (1)$$

where q_t is the adsorption capacity at time t (mg/g), V is the MB solution volume (l), C_0 is initial MB concentration (mg/l), C_t is the concentration of the MB solution at time t (mg/l), and m is the mass of adsorbent (g).

The percentage of adsorption can be calculated as follows:

$$\%A = \frac{C_0 - C_t}{C_0} \times 100. \quad (2)$$

Results and Discussion

Characterization of adsorbents

The morphological characteristics of the samples were revealed by SEM. The SEM images of VA and TVA catalysts are displayed in Figure 1. The SEM images corresponding to VAs (Figures 1a, b) confirm the relatively high porous structure of this substrate, which is composed mainly by particles with irregular shapes in the range of 0.2–2 μm . For the Ti-loaded samples, the SEM images in Figures 1c–f show the presence of quite regular TiO_2 microspheres (ca. 5 μm) (Figures 1c, d). In the junction zones between microspheres and the nanoscales bed, a few nanorose-like shapes arranged in a radial symmetry can be discerned (Figure 1e). At high magnifications, the presence of nanoneedles with a diameter around 50 nm can also be detected on the microspheres surface (Figure 1f).

The nitrogen adsorption–desorption isotherms of VA and TVA samples belong to Type IV of BDDT classification; they are concave to the relative pressure axis and present a

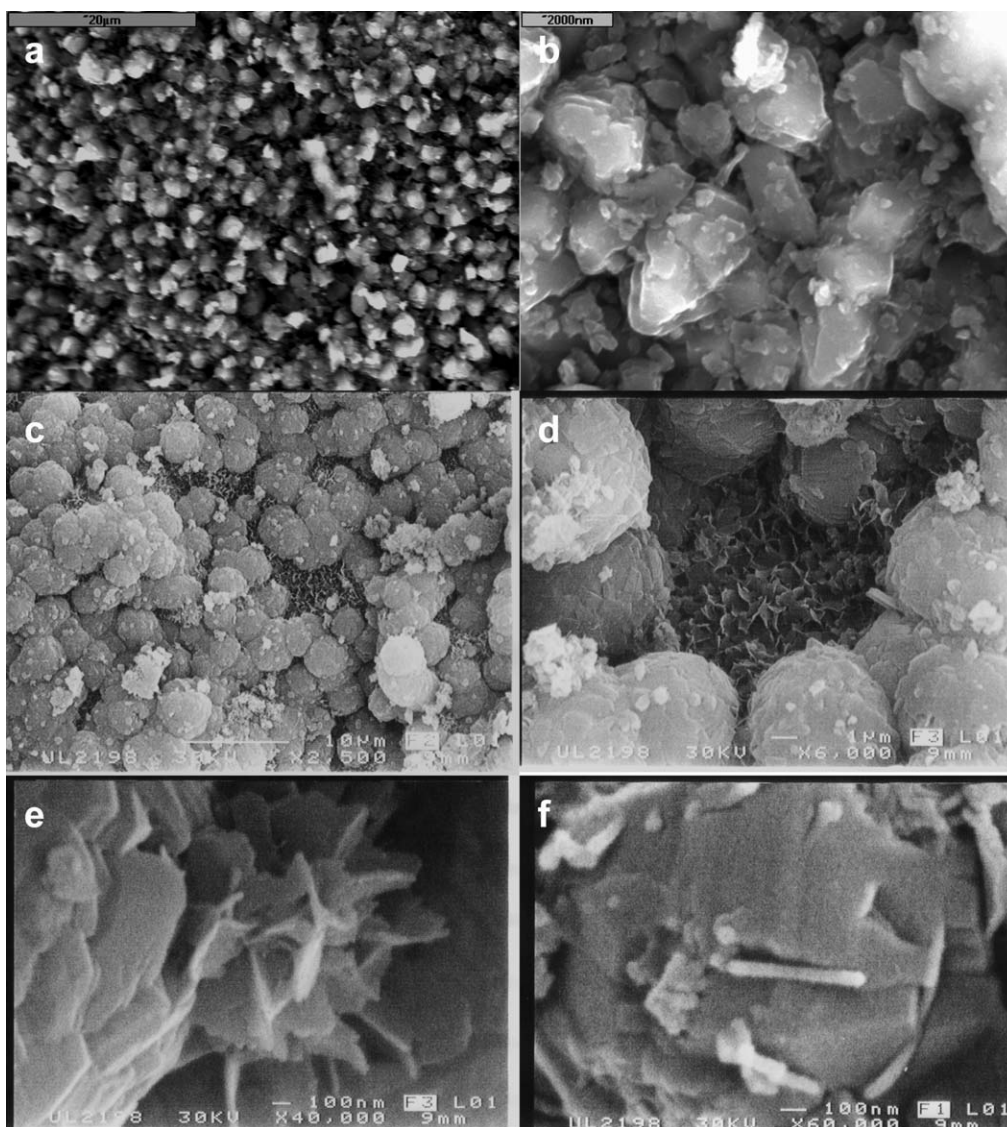


Figure 1. SEM images.

(a, b) Natural volcanic ashes and (c–f) titanated volcanic ashes.

hysteresis loop, which is commonly associated with the presence of mesoporosity. Specific areas were calculated by applying the Brunauer-Emmett-Teller (BET) equation to the equilibrium adsorption data within the range 0.05–0.28 of relative pressures. The total pore volume was estimated as the volume of liquid nitrogen at a relative pressure of around 0.98. The micropore volume and pore size were determined from the desorption branch of the isotherm using the Barrett-Joyner-Halenda method. The values of BET surface area, total pore volume of pores, and average pore diameter for VA and TVA, respectively, are as follows: 5.7–33.0 m²/g, 0.013–0.085 cm³/g, and 9.3–10.3 nm.

Effect of pH

As MB is a cationic dye, the extent of adsorption onto the adsorbent surface is expected to be dependent on the pH of the dye solution. Figure 2 shows the influence of pH on the

equilibrium adsorption value of the MB dye on both VA and TVA substrates. The common trend observed is that the extent of MB adsorption on both VA and TVA samples increases upon increasing pH values. This behavior can be explained in terms of the electrostatic forces developed on a negatively charged surface when pH increases and the cationic dye present in the solution. In addition, from the data reported in this figure, it is clear that Ti loading on the VA substrate according to the hydrothermal method enhances markedly the extent of MB adsorption at 20°C along the whole explored pH = 3–10 range. A similar result was reported for the adsorption of MB from aqueous solution by hazelnut shell²⁹ finding quite different kinetic adsorption curves slopes in the region below 120 min. Whatever pH, the kinetic adsorption curves for VA samples reach saturation at adsorption times below 40 min; however, longer times (~120 min) are required to reach the equilibrium of adsorption for TVA samples. This behavior can be related to

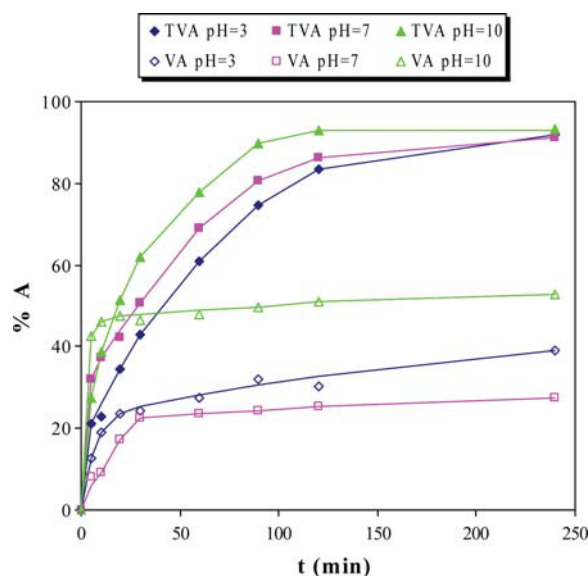


Figure 2. Effect of pH on the MB adsorption onto VA and TVA ($T = 20^{\circ}\text{C}$, $C_0 = 20 \text{ mg/l}$, adsorbent dosage = 3 g/l , $V = 800 \text{ ml}$).

[Color figure can be viewed in the online issue, which is available at wileyonlinelibrary.com.]

MB molecules diffusion from bulk liquid toward TVA particles interface. For a better understanding of this phenomenon, kinetic adsorption curves on TVA samples were recorded at various MB concentrations.

Effect of initial concentration

The effect of the initial concentration was studied for TVA because this substrate displayed higher extent of MB adsorption than the original VA counterpart. TVA adsorption capacity was studied as a function of initial dye concentration. The data collected in Figure 3 indicate, in accordance with literature, that dye removal is strongly dependent on initial dye solution concentration.^{20,34} As can be seen that time required to reach adsorption equilibrium is rather low for dilute MB solutions; however, longer equilibrium times are observed for higher MB dye concentrations. This behavior can be interpreted assuming that there is enough easily accessible surface area to accommodate most of the adsorbate at low concentration, and the measurement resolution is not sufficient to see very small concentration changes at longer times.

Effect of adsorbent dosage

Adsorbent dosage is an important parameter to evaluate the capacity of an adsorbent for a given initial adsorbate concentration. Figure 4 shows the effect of TVA dosage on MB removal keeping constant values for all other experimental conditions. The adsorption percentage (%A) increases with increasing the adsorbent dosage because the adsorbent surface area also increases, resulting in more adsorption sites available. However, at high adsorbent dosage, the dye adsorption was almost constant. It is basically due to adsorption sites remaining unsaturated during the adsorption reaction. In these conditions, the optimal adsorbent dosage was found to be close to 3 g/l .

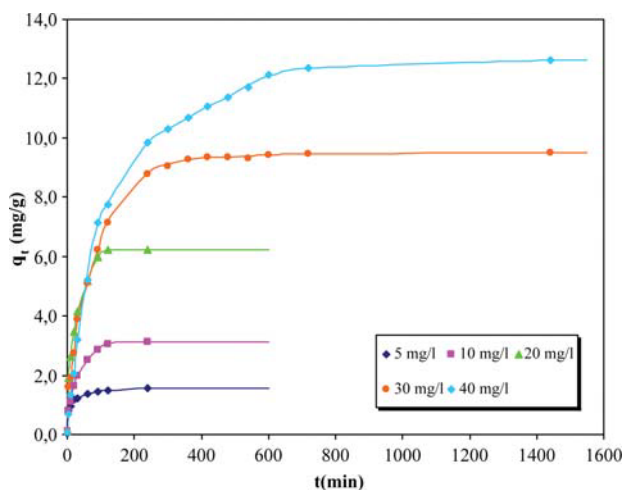


Figure 3. Effect of initial concentration on the MB adsorption onto TVA ($T = 20^{\circ}\text{C}$, $\text{pH} = 10$, adsorbent dosage = 3 g/l , $V = 800 \text{ ml}$).

[Color figure can be viewed in the online issue, which is available at wileyonlinelibrary.com.]

MB adsorption isotherms

A study of the equilibrium adsorption isotherm provides information about the mechanism of adsorption, which is important for the efficiency of the process and for the design of adsorption systems. In general, the adsorption isotherm describes how adsorbates interact with adsorbents and thus it is critical in optimizing the use of adsorbents. Among the various equilibrium adsorption isotherms available, only the Langmuir and Freundlich models were considered in this study: (i) the Langmuir and (ii) the Freundlich isotherms.²⁰

The Langmuir adsorption isotherm assumes that adsorption takes place at specific homogeneous sites within the adsorbent. This isotherm has been used successfully to describe many processes of adsorbate coverage below the monolayer adsorption capacity. The Langmuir model can be represented as follows³⁵:

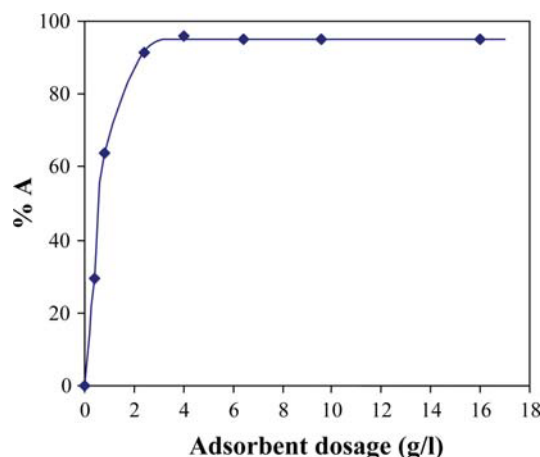


Figure 4. Effect of adsorbent dosage on the MB adsorption onto TVA ($T = 20^{\circ}\text{C}$, $C_0 = 20 \text{ mg/l}$, $V = 800 \text{ ml}$, contact time = 240 min).

[Color figure can be viewed in the online issue, which is available at wileyonlinelibrary.com.]

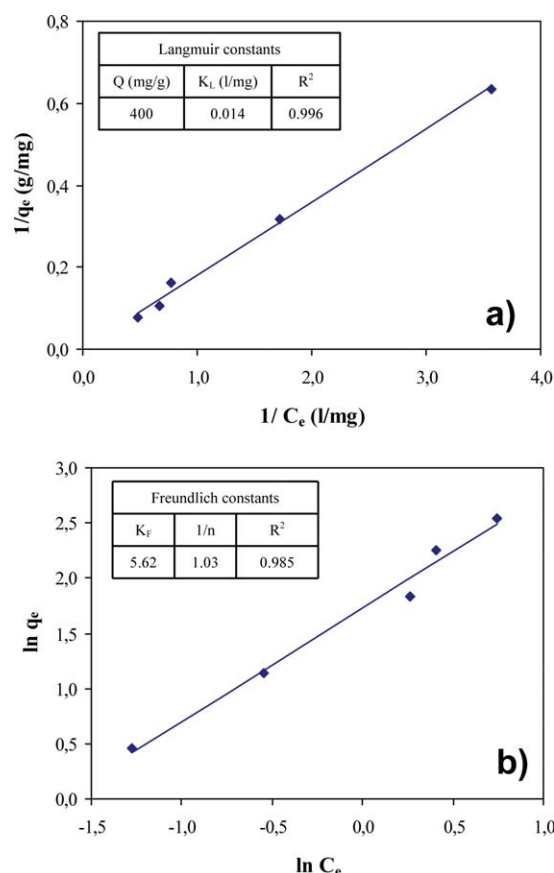


Figure 5. (a) Langmuir isotherm and (b) Freundlich isotherm for MB adsorption onto TVA.

[Color figure can be viewed in the online issue, which is available at wileyonlinelibrary.com.]

$$q_e = \frac{QK_L C_e}{1 + K_L C_e}, \quad (4)$$

where q_e is the equilibrium adsorption capacity (mg/g), C_e is the equilibrium concentration of the MB solution (mg/l), Q is the capacity of MB adsorbed at complete monolayer coverage (mg/g), and K_L is the Langmuir constant (l/mg). The equation can be linearized as follows:

$$\frac{1}{q_e} = \frac{1}{Q} + \frac{1}{K_L Q} \frac{1}{C_e}. \quad (5)$$

In Eq. 5, the values of Q and K_L can be calculated from plotting experimental values of $1/q_e$ vs. $1/C_e$.

The Freundlich isotherm is often used to describe the adsorption of a given adsorbate on a heterogeneous surface in which there is a distribution of adsorption energies. The Freundlich model adopts the following form³⁵:

$$q_e = K_F C_e^{1/n}. \quad (6)$$

In which K_F is called the Freundlich constant (mg/g (mg/l)^{1/n}) and $1/n$ is the heterogeneity factor. Equation 6 can be linearized by taking natural logarithms:

$$\ln q_e = \ln K_F + \frac{1}{n} \ln C_e. \quad (7)$$

In Eq. 7, K_F and $1/n$ can be determined from the linear plot of $\ln q_e$ vs. $\ln C_e$.

Figures 5a, b show Langmuir and Freundlich adsorption isotherms obtained for TVA material, respectively. Apparently, both isotherms fit experimental data; however, a low standard deviation can be observed when using the Langmuir equation. The calculated Langmuir and Freundlich constants derived from the fit of experimental data to Eqs. 5 and 7 are showed in Figures 5a, b. As the Langmuir isotherm assumes uniformity in the adsorption heats, it could be inferred that the distribution of the adsorption energy is rather narrow.

The adsorption capacity of different types of adsorbent used for MB removal from literature is summarized in Table 1. The value of Q obtained in this study (400 mg/g) is larger than that found in most previous works. This suggests that TVA substrate is a good candidate to be used in the removal of MB from aqueous waste streams.

MB adsorption kinetics

Kinetic study is one of the most important methods to evaluate the efficiency of adsorption. Two kinetic models, pseudo-first-order and pseudo-second-order, were adopted to investigate the adsorption processes of MB on the TVA substrate.

Pseudo-first-order model

A linear form of pseudo-first-order kinetic model was described by Lagergren⁴¹:

$$\ln(q_e - q_t) = \ln q_e - k_1 t, \quad (8)$$

where q_e and q_t are the amounts of MB adsorbed (mg/g) at equilibrium and at time t (min), respectively, and k_1 is the rate constant of the pseudo-first-order adsorption kinetics (min⁻¹). The validity of the model can be checked by plotting $\ln(q_e -$

Table 1. Adsorption Capacity of Different Adsorbents for MB Adsorption

Adsorbents	BET Surface Area (m ² /g)	Adsorption Capacity Q (mg/g)	Ref.
Acid-treated zeolite	764	262.87	3
Alkaline-treated zeolite	936	436.55	3
Bamboo-based activated carbon	1896	454.20	36
Bamboo dust activated carbon	—	143.20	37
Groundnut shell activated carbon	—	164.90	37
Rice husk	—	40.59	16
Wheat shells	0.67	21.50	20
Natural zeolite	—	29.18	27
Fly ash	6.52	5.57	28
Tea waste	—	85.16	30
Silica	7.4	11.21	38
Glass fibers	—	2.24	39
Coir pith	—	120.43	40
Titanated volcanic ashes	33.0	400.00	This study

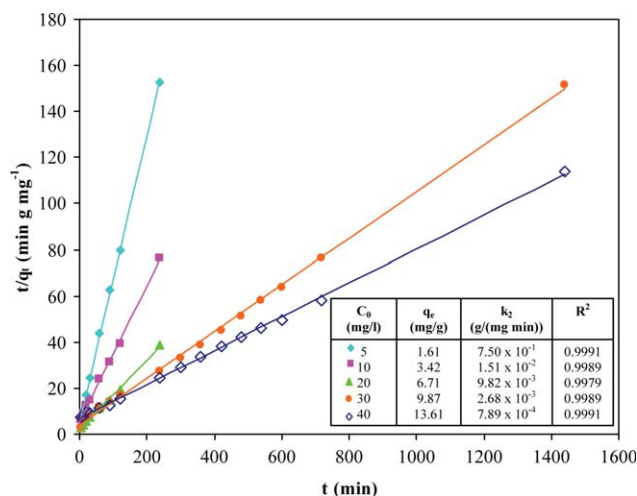


Figure 6. Pseudo-second-order adsorption kinetics of MB adsorption onto TVA ($T = 20^\circ\text{C}$, $C_0 = 5, 10, 20, 30$, and 40 mg/l, adsorbent dosage = 3 g/l, $\text{pH} = 10$, $V = 800$ ml).

[Color figure can be viewed in the online issue, which is available at wileyonlinelibrary.com.]

q_t) vs. t . The rate constant of pseudo-first-order adsorption can be determined from the slope of the plot. The fit of experimental results obtained by plotting $\ln(q_e - q_t)$ vs. t (not shown here) did not show a straight line during the whole adsorption process, indicating that pseudo-first-order kinetics does not describe the adsorption behaviors of MB onto the TVA substrate.

Pseudo-second-order model

The pseudo-second-order kinetic model can be represented in linear form as follows⁴¹:

$$\frac{t}{q_t} = \frac{1}{k_2 q_e^2} + \frac{1}{q_e} t, \quad (9)$$

where k_2 is the rate constant of the pseudo-second-order adsorption kinetics (g/mg min). The q_e and k_2 can be obtained from the slope and the intercept of plots of t/q_t vs. t .

Figure 6 shows the plots of t/q_t vs. t based on pseudo-second-order kinetics. According to this model, straight lines were obtained; the standard deviation in all cases was better than 0.99, indicating that MB adsorption onto TVA kinetics can be satisfactorily described by a pseudo-second-order kinetics model. Moreover, this figure shows the parameters of pseudo-second-order kinetics for different MB initial concentration solutions. The MB equilibrium adsorption capacities predicted with this model, for each initial concentration solution, were similar to the experimental equilibrium adsorption capacities founded, represented in Figure 3.

Conclusions

The results presented in this work, about the kinetics and equilibrium of MB adsorption, show that VAs are good candidates to be used as adsorbents for the removal of this dye

from aqueous solutions. In particular, the TVAs exhibited higher adsorption of MB than the nontreated VA natural material. Both Langmuir and Freundlich adsorption isotherm models were applied to describe MB equilibrium adsorption data onto TVA substrate at 20°C , providing a better fit for the Langmuir isotherm model. The maximum adsorption capacity of the dye was found to be 0.40 g of the MB dye per gram of TVA, which is larger than most of the values found in most previous works in bibliography for several adsorbent materials. MB adsorption on TVA substrate kinetics can be satisfactorily described by a pseudo-second-order kinetics model. Adsorption loading increased with increasing pH in the range of pH 3–10, and the optimum conditions for the adsorption process were found using an adsorbent dose of 3 g/l.

Literature Cited

- Malik PK. Use of activated carbon prepared from sawdust and rice-husk for adsorption of acid dyes: a case study of Yellow 36. *Dyes Pigments*. 2003;56:239–249.
- Attia AA, Girgis BS, Fathy NA. Removal of methylene blue by carbons derived from peach stones by H_3PO_4 activation: batch and column studies. *Dyes Pigments*. 2008;76:282–289.
- Yang C, Wang C, Yao J, Zhang L, Liu X. Adsorption of methylene blue on mesoporous carbons prepared using acid- and alkaline-treated zeolite X as the template. *Colloids Surf A: Physicochem Eng Aspects*. 2009;333:115–119.
- Baskaralingam P, Pulikesi M, Elango D, Ramamurthi V, Sivasenan S. Adsorption of acid dye onto organobentonite. *J Hazard Mater*. 2006;128:138–144.
- Allen SJ, Koumanova B. Decolourisation of water/wastewater using adsorption (review). *J Univ Chem Technol Metall*. 2005;40:175–192.
- Asem AA, Ahmed MD, Waheeba AA. Adsorption/desorption behavior of acid orange 10 on magnetic silica modified with amine groups. *Chem Eng J*. 2009;150:55–62.
- Gomez V, Larrechi MS, Callao MP. Kinetic and adsorption study of acid dye removal using activated carbon. *Chemosphere*. 2007;69:1151–1158.
- Tan IAW, Hameed BH, Ahmad AL. Equilibrium and kinetic studies on basic dye adsorption by oil palm fibre activated carbon. *Chem Eng J*. 2007;127:111–119.
- Iqbal MJ, Ashiq MN. Adsorption of dyes from aqueous solutions on activated charcoal. *J Hazard Mater*. 2007;139:57–66.
- Tseng RL, Tseng SK. Pore structure and adsorption performance of the KOH-activated carbons prepared from corncob. *J Colloid Interface Sci*. 2005;287:428–437.
- Zhang J, Shi Q, Zhang C, Xu J, Zhai B, Zhang B. Adsorption of Neutral Red onto Mn-impregnated activated carbons prepared from *Typha orientalis*. *Bioresour Technol*. 2008;99:8974–8980.
- Wang S, Boyjoo Y, Choueib A. A comparative study of dye removal using fly ash treated by different methods. *Chemosphere*. 2005;60:1401–1407.
- Akbal F. Adsorption of basic dyes from aqueous solution onto pumice powder. *J Colloid Interface Sci*. 2005;286:455–458.
- Gücek A, Şener S, Bilgen S, Mazmancı MA. Adsorption and kinetic studies of cationic and anionic dyes on pyrophyllite from aqueous solutions. *J Colloid Interface Sci*. 2005;286:53–60.
- Dogan M, Alkan M, Türkyılmaz A, Özdemir Y. Kinetics and mechanism of removal of methylene blue by adsorption onto perlite. *J Hazard Mater*. 2004;109:141–148.
- Vadivelan V, Kumar KV. Equilibrium, kinetics, mechanism, and process design for the sorption of methylene blue onto rice husk. *J Colloid Interface Sci*. 2005;286:90–100.
- Rauf MA, Shehadi I, Hassan WW. Studies on the removal of neutral red on sand from aqueous solution and its kinetic behaviour. *Dyes Pigments*. 2007;75:723–726.
- Lehocky M, Mracek A. Improvement of dye adsorption on synthetic polyester fibers by low temperature plasma pre-treatment. *Czech J Phys*. 2006;56:1277–1282.

19. Harris RG, Wells JD, Johnson BB. Selective adsorption of dyes and other organic molecules to kaolinite and oxide surfaces. *Colloids Surf A: Physicochem Eng Aspects*. 2001;180:131–140.
20. Bulut Y, Aydın H. A kinetics and thermodynamics study of methylene blue adsorption on wheat shells. *Desalination*. 2006;194:259–267.
21. Wang S, Zhu ZH, Coomes A, Haghseresht F, Lu GQ. The physical and surface chemical characteristics of activated carbons and the sorption of methylene blue from wastewater. *J Colloid Interface Sci*. 2005;284:440–446.
22. Kumar KV, Sivanesan S. Equilibrium data, isotherm parameters and process design for partial and complete isotherm of methylene blue onto activated carbon. *J Hazard Mater*. 2006;134:237–244.
23. Kumar KV. Linear and non-linear regression analysis for the sorption kinetics of methylene blue onto activated carbon. *J Hazard Mater*. 2006;137:1538–1544.
24. Potgieter JH. An experimental study of the adsorption behaviour of methylene blue on activated carbon. *Colloids Surf*. 1990;50:39–399.
25. Barton SS. The adsorption of methylene blue by activated carbon. *Carbon*. 1987;25:3432–4350.
26. Avom J, Mbadcam JK, Noubactep C, Germain P. Adsorption of methylene blue from an aqueous solution onto activated carbon from palm-tree cobs. *Carbon*. 1997;35:365–369.
27. Han R, Zhang J, Han P, Wang Y, Zhao Z, Tang M. Study of equilibrium, kinetic and thermodynamic parameters about methylene blue adsorption onto natural zeolite. *Chem Eng J*. 2009;145:496–504.
28. Kumar KV, Ramamurthi V, Sivanesan S. Modeling the mechanism involved during the sorption of methylene blue onto fly ash. *J Colloid Interface Sci*. 2005;284:14–21.
29. Dogan M, Abak H, Alkan M. Adsorption of methylene blue onto hazelnut shell: kinetics, mechanism and activation parameters. *J Hazard Mater*. 2009;164:172–181.
30. Tamez Uddin Md, Akhtarul Islam Md, Mahmud Sh, Rukanuzzaman Md. Adsorptive removal of methylene blue by tea waste. *J Hazard Mater*. 2009;164:53–60.
31. Borges ME, Alvarez-Galván MC, Esparza P, Medina E, Martín-Zarza P, Fierro J. Ti-containing volcanic ash photocatalyst for degradation of phenol. *Energy Environ Sci*. 2008;1:364–369.
32. Inagaki M, Kondo N, Nonaka R, Ito E, Toyoda M, Sogabe K, Tsunuma T. Structure and photoactivity of titania derived from nanotubes and nanofibers. *J Hazard Mater*. 2009;161:1514–1521.
33. Hsieh C, Fan W, Chen W. Impact of mesoporous pore distribution on adsorption of methylene blue onto titania nanotubes in aqueous solution. *Microporous Mesoporous Mater*. 2008;116:677–683.
34. Rauf MA, Qadri SM, Ashraf S, Al-Mansoori KM. Adsorption studies of Toluidine Blue from aqueous solutions onto gypsum. *Chem Eng J*. 2008;150:90–95.
35. Hameed BH, Salman JM, Ahmad AL. Adsorption isotherm and kinetic modelling of 2,4-D pesticide on activated carbon derived from date stones. *J Hazard Mater*. 2009;163:121–126.
36. Hameed BH, Din ATM, Ahmad AL. Adsorption of methylene blue onto bamboo-based activated carbon: kinetics and equilibrium studies. *J Hazard Mater*. 2007;141:819–825.
37. Kannan N, Sundaram MM. Kinetics and mechanism of removal of methylene blue by adsorption on various carbons—a comparative study. *Dyes Pigments*. 2001;51:25–40.
38. Woolard CD, Strong J, Erasmus CR. Evaluation of the use of modified coal ash as a potential sorbent for organic waste streams. *Appl Geochem*. 2002;17:1159–1164.
39. Chakrabarti S, Dutta BK. On the adsorption and diffusion of methylene blue in glass fibers. *J Colloid Interface Sci*. 2005;286:807–811.
40. Namasivayam C, Radhika R, Suba S. Uptake of dyes by a promising locally available agricultural solid waste: coir pith. *Waste Manage*. 2001;21:381–387.
41. Cheung WH, Szeto YS, McKay G. Enhancing the adsorption capacities of acid dyes by chitosan nano particles. *Bioresour Technol*. 2009;100:1143–1148.

Manuscript received Dec. 23, 2009, and revision received Apr. 16, 2010.